Helical zinc complexes of pyrazine–pyridine hybrids

S.I.G. Dias [a], Fenton Heirtzler [a,*], T. Bark [b], Gael Labat [c], Antonia Neels [c]

[a] *School of Physical Sciences, Chemical Laboratory, University of Kent, Canterbury, Kent CT2 7NH, UK*
[b] *Department of Chemistry, University of Fribourg, Pérolles, 1700 Fribourg, Switzerland*
[c] *Institute of Chemistry, University of Neuchâtel, Avenue de Bellevaux 51, 2000 Neuchâtel, Switzerland*

Abstract

The zinc(II) complexes **1a**ZnCl$_2$ and **1b**ZnCl$_2$ (**1a**: 2-(6′,2″-bipyrid-2′-yl)-3-(2-pyridyl)pyrazine; **1b**: 2-(6′,2′-bipyrid-2′-yl)-5,6-di-nitrilo-3-(2-pyridyl)pyrazine) were prepared by treatment of the ligands with ZnCl$_2$. The structures of both were investigated by X-ray crystallography and ^{1}H NMR spectroscopy. Both complexes display proton deshielding phenomena that are attributed to a twisted solution-state molecular conformation. In the solid state, **1a**ZnCl$_2$ exhibits a high degree of torsion about the axis through the uncomplexed pyridine ring and the pendant chlorine atoms. The solid-state structure and solution-state self-associative behavior of **1b**ZnCl$_2$ are indicative of a partial self-assembly motif.

Keywords: Pyrazine; Pyridine; X-ray; NMR; Stacking; Twist

1. Introduction

Recently, we described several examples of so-called pyrazine–pyridine hybrids, which self-assemble with particular metal salts to π-stacked, dimeric complexes [1–4]. In unsymmetrical ligands such as **1a**, the 2,3-disubstitution pattern of oligopyridyl chains on the pyrazine ring [5–8] is decisive in a preference for tetrahedral metals [2–4]. The angular arrangement of divergent binding sites leads to a bis-bidentate, instead of bidentate/terdentate complexation mode (Fig. 1). Such complexes also organize through homopyrazine π-stacking, affording a chiral, $\Delta\Delta/\Lambda\Lambda$-configuration, and via the solid-state π-stacking of metallo-cyclophane cations, to provide a high degree of parallel lattice ordering [4,7]. In the native ligands, twisting interactions induce a single-helical molecular conformation [7].

Metallo-organic supramolecular complexes of zinc(II) and oligopyridine-type ligands are attracting attention on account of their excellent excited-state dipolar properties, which render them relevant to ap-plications based on non-linear optical effects [9–12]. These bulk properties can be enhanced through incorporation into highly ordered and polar lattices [12–16]. Symmetrical 2,5-dipyridylpyrazine-type ligands and their 2,6′-bipyridyl homologues self-assemble with zinc(II) salts to linear or bridged polymeric as well as macrocyclic-polymetallic structures and through which stereochemical and chiral features may be efficiently expressed [17,18]. Whereas single-enantiomer chirality is an additional means of organizing transition dipole moments, i.e., via non-centrosymmetric crystal-lattice ordering [16,19], so far equilibrating mixtures of *meso*/chiral metallo-cyclophanes containing octahedral di-zinc(II) have been reported [20,21]. Thus, we were attracted to the use of zinc(II) metallo-cyclophanes and related complexes as novel metallo-organic photonic materials. Preliminary work dictated examining the currently available 2,3-disubstituted ligands' interaction with practical zinc(II) salts, with an emphasis on coordination [22] and ligand geometry, intra/intermolecular stacking effects and long-range interactions. Since the synthesis of analogous 2,3-dicyanopyrazine ligands is possible through our previously-introduced methodology [8], and nitrile substitution increases dipolar alignment [23–26], these materials were also of interest.

---

* Corresponding author. Tel.: +44-1227-827-041; fax: +44-1227-827-724.

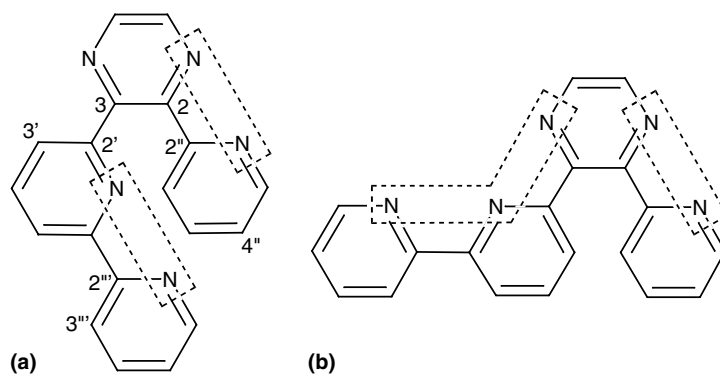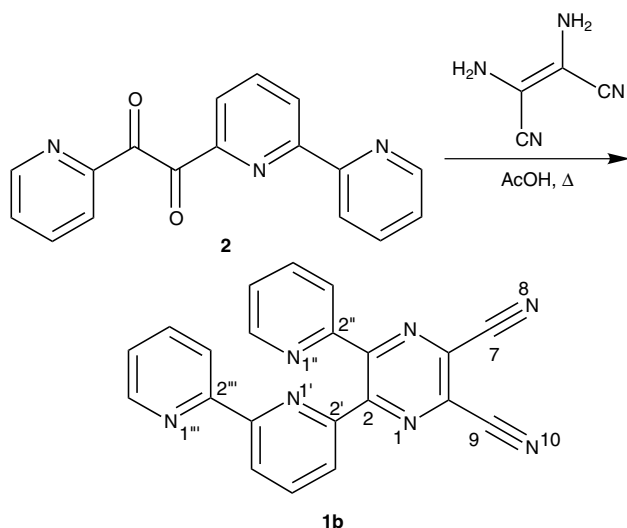*E-mail address:* heirtzler@web.de (F. Heirtzler).

1

Fig. 1. Potential binding domains in ligand **1a**.

2. Results and discussion

Ligand **1a** was available from earlier studies [7]. Heating of the unsymmetrical α-diketone **2** [8] with one equivalent of diaminomaleonitrile in glacial acetic acid afforded dinitrile-substituted ligand **1b** in 67% yield after purification (Scheme 1). Treatment of **1a** and **1b** with zinc dichloride in acetonitrile or acetonitrile-chloroform under reflux conditions resulted in the precipitation of sparingly-soluble solids that could be recrystallized from hot nitromethane. The results of combustion analyses on these complexes were in agreement with a 1:1:2 stoichiometry of **1a/1b**:Zn:Cl. While the electrospray- and FAB-mass spectra of both complexes displayed m/z signals of monomeric materials, the base signal of the complex from **1b** corresponded to $[\mathbf{1b}_2Zn]^+$. There was thus just cause to investigate their solid-state structures through X-ray crystal structure analysis, as well as to clarify their organizational priorities (see Section 4 for full details).

The complexation domain of **1aZnCl₂** contains η^3-coordination of **1a** to the metal and has a monomeric

Scheme 1. Synthesis of nitrile disubstituted **1b**.

constitution (Fig. 2(a)). The metal-nitrogen bond lengths (Table 1) and deviations of the constituent aza-aromatics from co-planarity are indicative of a lopsided terdentate coordination. In particular, the Zn–N lengths to pyridine are shorter than to pyrazine, and the torsional angle between C_5H_3N pyridine and pyrazine is significantly greater than that between the adjacent pyridine rings. The pendant chlorine atoms occupy pseudo-axial positions. While the zinc–chlorine bonding distances are unremarkable, the halogens' orientation with respect to the overall molecular geometry warrants comment. One of these, Cl1, is within 0.05 Å of the mean plane of the C_5H_3N ring, while the other (Cl2) lies 3.04 Å on the other side of the same plane. The zinc–chlorine bond angles to nitrogen of C_5H_3N are correspondingly deformed. The uncomplexed pyridine ring is twisted with respect to and deflected out of the plane of the pyrazine ring. Both of the pyridyl–pyrazine torsions occur at the cost of atomic deviations from the mean plane of pyrazine (0.01–0.09 Å). The location of the uncomplexed C_5H_4N ring on the opposite side to Cl2 gives the entire molecule a shallow helical pitch.

Two different intermolecular parallel stacking interactions are apparent in the lattice of **1aZnCl₂**. The complexed bipyridyl domains stack in offset, anti-parallel pairs related by an inversion center (Fig. 2(b)). Thus, while the individually stacking C_5H_4N and C_5H_3N rings are canted 9.83° overall, the bipyridyl rings are co-planar, with atomic distances from the respective mean ring planes in the 3.14–3.81 Å range. Also, columns of homochiral helices are interdigitated by their racemates (Fig. 2(c)). This interpenetration occurs via anti-parallel pyridylpyrazine stacking interactions, which besides minimizing contact between the $ZnCl_2$ centers, generates an inversion center between them. Short H···Cl contacts [27] to the uncomplexed pyridine ring (Cl1···H5‴ and Cl2···H4‴) between the interdigitating columns are apparent.

The complex **1bZnCl₂** is surprisingly monomeric, and occurs as a solvate with a 2:1 – ratio of nitromethane to complex. Strikingly, layers of nitromethane are sepa-
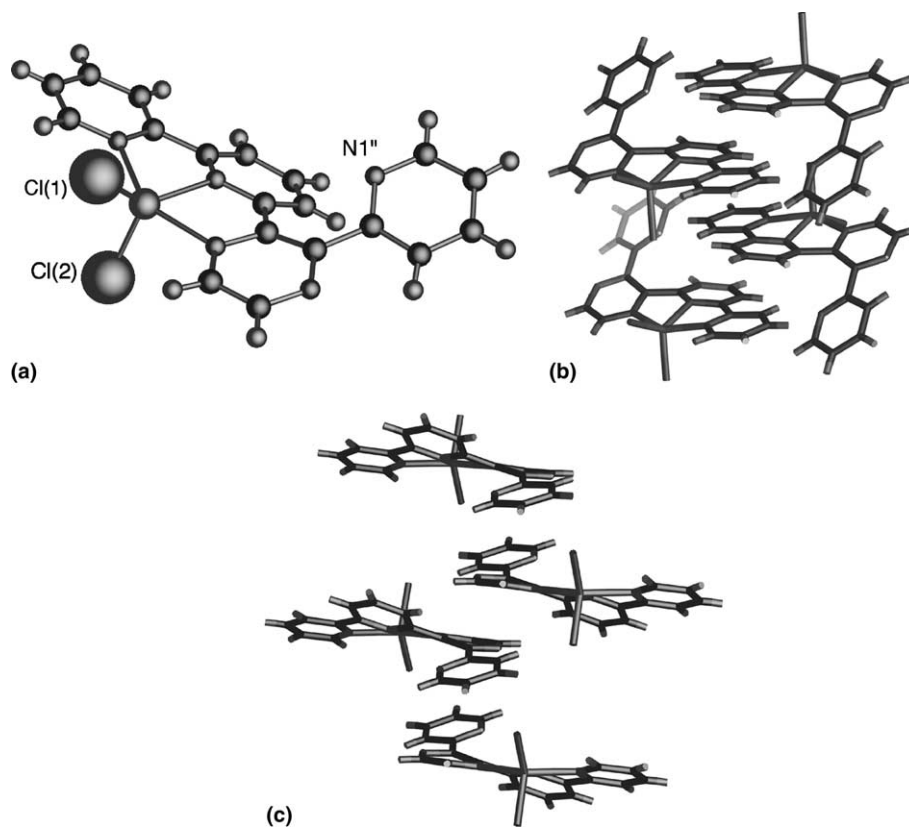
Fig. 2. Crystal structure of complex **1a**ZnCl$_2$: (a) single molecule, emphasizing twist with respect to N(1″) pyridine ring; (b) parallel stacking of complexed 2,6′-bipyridyl domains; (c) mirror-image columns of stacked 3-(2′-pyridyl)pyrazine subunits.

Table 1
Bonding- and non-bonding parameters associated with **1a**ZnCl$_2$ and **1b**ZnCl$_2$

Substance	**1a**ZnCl$_2$	**1b**ZnCl$_2$	Substance	**1a**ZnCl$_2$	**1b**ZnCl$_2$
Bond lengths			*Distances from mean plane:*		
N(1)–Zn	2.2175 Å	2.523 Å	Cl(1)–C$_5$H$_3$N	0.048 Å	1.761 Å
N(1′)–Zn	2.1120 Å	2.074 Å	Cl(2)–C$_5$H$_3$N	−3.042 Å	−1.983 Å
N(1‴)–Zn	2.1668 Å	2.097 Å			
Cl(1)–Zn	2.2411 Å	2.2116 Å	*Extra-annular torsional angles:*		
Cl(2)–Zn	2.2784 Å	2.2215 Å	Pyrazine-C$_5$H$_3$N	28.61°	22.618°
			C$_5$H$_3$N–C$_5$H$_4$N	9.83°	1.294°
Bond angles			Pyrazine-C$_5$H$_4$N	22.35°	30.767
N(1)–Zn–N(1′)	73.570°	70.06°			
N(1′)–Zn–N(‴)	75.026°	78.05°			
N(1)–Zn–Cl(1)	98.179°	93.01°			
N(1′)–Zn–Cl(1)	136.994°	112.02°			
N(1‴)–Zn–Cl(1)	99.386°	108.43°			
N(1)–Zn–Cl(2)	98.043°	91.93°			
N(1′)–Zn–Cl(2)	108.721°	126.62°			
N(1‴)–Zn–Cl(2)	99.189°	99.25°			

rated by sheet-like **1b**ZnCl$_2$ complexation domains (Fig. 3(a)). The repeating distance between these two layers is ≈11.8 Å. While the complexation domain observed for **1b**ZnCl$_2$ superficially resembles that of **1a**ZnCl$_2$, significant differences in molecular geometry are apparent (Fig. 3(b)). An increased dissymmetry of the 2,2′:6′,2″-terpyridyl-like binding domain occurs, e.g. the Zn–N(1) (pyrazine) bond length increases by 14% relative to **1a**ZnCl$_2$ (Table 1). The origins of this effect

either plausibly involve electronic factors or steric interaction with chlorine atoms (closest contacts of Cl1 and Cl2 to nitrile carbons: 4.29 and 3.41 Å, respectively). The constituent atoms of the dicyanopyrazine ring deviate by 0.01–0.07 Å from their mean plane. This situation appears to reduce the overall ligand strain around the terdentate site, as reflected in extra-annular torsional angles. Deformation of the metal-halogen bonds with respect to the η^3-binding domain is relieved,
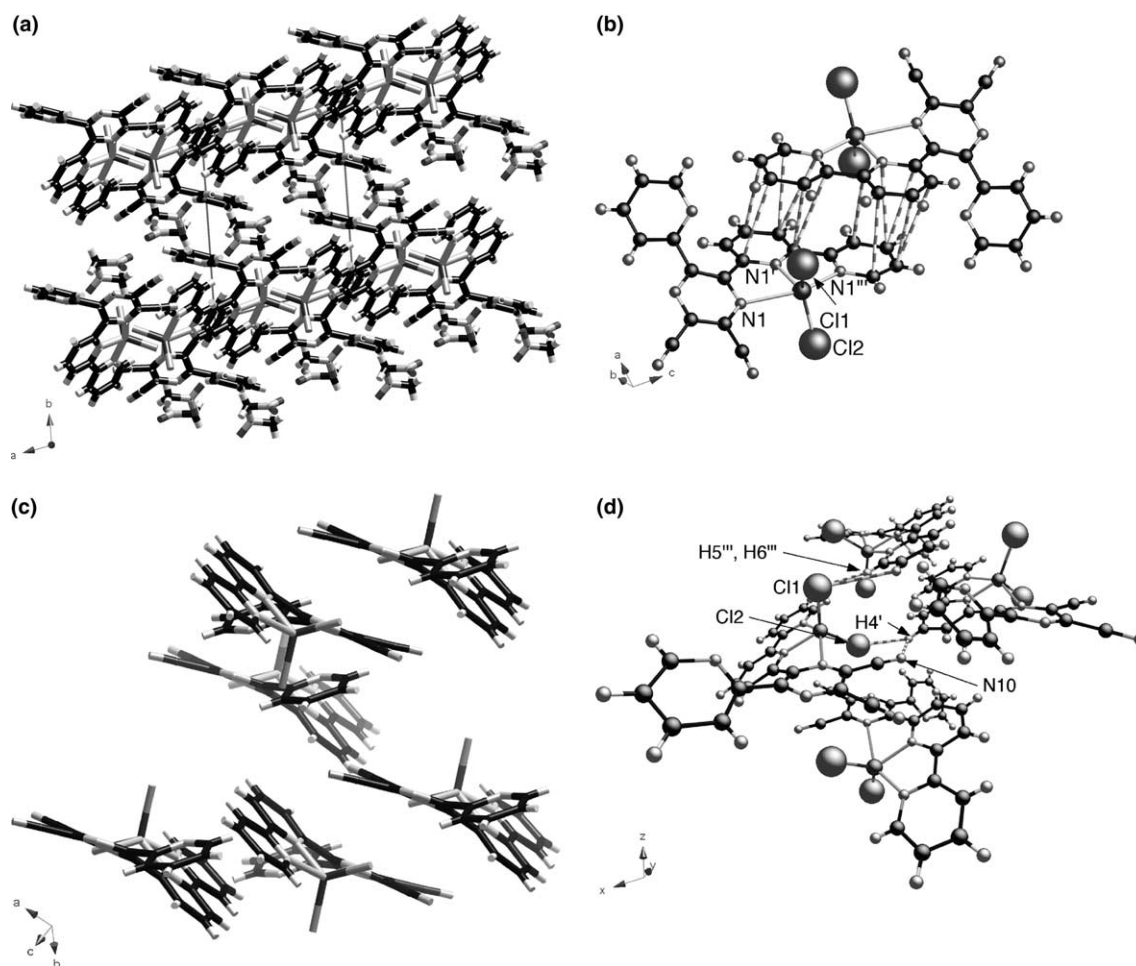
Fig. 3. Complex **1bZnCl₂** in the solid state: (a) alternating strata of complex and nitromethane; (b) stacked dimeric pairs; (c) stacked 3-(2′-pyridyl)pyrazine subunits [vertical orientation]; (d) likely close contacts.

as shown by the distances of the halogens from the mean plane of C_5H_3N pyridine. The bond angles and atom-to-plane distances involving N of C_5H_3N and the halogen atoms indicate that the Zn–Cl bond vectors are pointed marginally toward, and not away from the un-complexed C_5N_4N ring.

The most prominent intermolecular interaction of **1bZnCl₂** involves the stacking of inversion center-related pairs of bipyridyl sub-units in **1b** (Fig. 3(b)). These are coplanar to within 0.38° and are characterized by atom-to-mean plane distances in the 3.02–3.30 Å range and closest intermolecular atomic distances of 3.49–3.75 Å. Within this situation, the uncomplexed pyridine rings adapt, as in the case of **1aZnCl₂**, an approximately *anti*-conformation with respect to the pyrazine ring, but are intriguingly twisted inward towards their inversion-related stacking partners to afford estimated short inter-molecular N1″···H4‴ contacts of ~2.73 Å; no Cl···H distances within 3 Å are observed. Overall, the geometry and stacking interactions of this situation resemble those in the dicopper(I) metallo-cyclophane of **1a** (atom-to-plane stacking distances: 3.08–3.47 Å).

Another stacking interaction involves the synthon represented by the uncomplexed pyridylpyrazine fragment. This associates with itself to afford atom-to-plane separations and closest-neighbor distances (3.42–3.47 and 3.49–3.75 Å, respectively), bespeaking of an intermediate offset parallel stacking arrangement [28]. Each stacked pyridyl-pyrazinyl pair is coplanar to within 0.61°, although the individual stacking rings are tilted by 3.9° to each other.

Parallel alignment also occurs through the dicyano-pyrazine groups, that are oriented in an anti-parallel, dimeric manner (Fig. 3(c)). But also, the nitrile groups interconnect the closely stacked **1bZnCl₂** pairs from the opposite side of the dicyanopyrazine plane (Fig. 3(d)). For a given equivalent of **1bZnCl₂**, these involve short distances from both nitrile N10 and Cl2 to H4′, as well as Cl2···H5′, on a single molecular neighbor (2.78, 2.67 and 3.72 Å, respectively). Contacts from Cl1 to H5‴ and H6‴ on yet another adjoining molecule (3.56 and 3.11 Å) complete this aspect.

To compare the solid- and solution-state structures of the zinc complexes, their proton NMR spectra were

4

analysed and assigned. Since the ligand **1b** is previously unreported, its ^{1}H NMR spectrum deserves brief comment. The outstanding feature in this substance is the upfield resonance of H3$'''$, which is indicative of an edge-on-face stacking interaction between the spatially proximate C_5H_4N pyridine rings containing N1$'''$ and N1$''$ [7]. Thus, the presence of the nitrile groups does not interfere with the expected conformational preferences of this heterocyclic system. For the complexes, spectra were assigned with the assistance of pulse field gradient COSY spectra (Fig. 4). The downfield shift of H3$'''$ and its coupling constants are consistent with those of other terdentate pyridine–pyrazine complexes [29] and are indicative of complexation involving C_5H_4N pyridine of the 2,6$'$-bipyridyl substituent.

Also in both of the zinc(II) complexes, H3$''$ of C_5H_4N pyridine undergoes an unusual upfield shift (**1aZnCl$_2$** and **1bZnCl$_2$**: $\Delta\delta$ relative to ligands in CDCl$_3$: 0.51 δ 7.31 and 1.03, respectively). Initially, the assignment of the upfield doublet to H3$''$ (as opposed to H3$'$ of the C_5H_3N ring) was not straightforward. However, similar experiments on **1bZnCl$_2$** at 270 MHz clearly indicated the connectivity of this shift to the remaining three protons of the uncomplexed C_5H_4N ring. A similar shifting of this position occurs in dimeric metallo-cyclophanes, but in that case arises from an edge-on-face interaction of the orthogonally directed bipyridyl complexation domains [2,3]. Insight into the origins of this new effect is provided through molecular model studies. Orthogonal stacking of the uncomplexed C_5H_4N pyridine ring against the C_5H_3N ring should induce a shielding effect in spatially adjacent positions in the later, but not the former ring. However, other η^3-metalloorganic complexes of 2,3-disubstituted pyrazine–pyridine hybrids exist in highly twisted solution-state

geometries [29,30], suggesting that long-range effects, to cause shielding of H3$''$ by the chlorine atoms, may occur for the current zinc(II) complexes. Since, however no dynamic signal broadening width was observed at 25 °C, any such fluxional processes involving the uncomplexed pyridine ring are rapid on the ^{1}H NMR spectroscopic time scale.

3. Concluding remarks

Complexation of the sterically hindered bipyridyl-pyridylpyrazine hybrids **1a** and **1b** with zinc(II) induces a change from bis-bidentate to terdentate complexation geometry, while maintaining related long-range stacking and organizational features as for dimeric metallo-cyclophanes. Tantalizingly, the appearance of mass spectral signals from [**1b$_2$Zn**]$^+$, the weakened Zn–N (pyrazine) bond and the dimeric, multi-interaction solid-state stacking motif of **1bZnCl$_2$** suggest that this complex is on the brink of an oligomeric self-assembly program. For both new complexes, solid-state atropisomeric chirality in the form of helicity is observed, and is also probable in solution, a feature that compliments the point chirality of the metallo-cyclophanes. Thus, the precise molecular and crystal lattice topology can be controlled through appropriate substitution of the ligand scaffolding. Indeed, highly polar nitrile substitution, which is desirable from the point of excited-state dipole moment tuning, is tolerated by the observed complexation mode. These studies have revealed to us the complexity of the organizational and topological phenomena possible for such pyrazine–pyridine hybrids, and will aid in the design of monomeric and dimeric zinc(II) complexes appropriate for evaluation excited-state dipolar properties.

4. Experimental

4.1. General procedures and starting materials

Electrospray mass spectra (ES-MS) were recorded on a ThermoFinnigan LCQ Classic by direct injection into a flow of acetonitrile at 5 µl/min, needle voltage 3.5 kV, capillary voltage 30 V and capillary temperature 60 °C. Data was collected manually in Tune Plus and visualised in the Qual Browser of the Excalibur software. FAB-MS spectra were recorded on a VG Instruments 7070E instrument with a FAB inlet system. Infrared spectra were recorded in a Mattson FT-IR spectrometer as KBr disks. UV spectra were recorded on a Unicam apparatus. Elementary analyses were obtained in a Carlo Erba Elemental Analyser. ^{1}H NMR spectra were recorded at 25 °C on Jeol 270 GSX and Bruker Avance 400 spectrometers. ^{13}C NMR spectra were recorded at 67.5 MHz
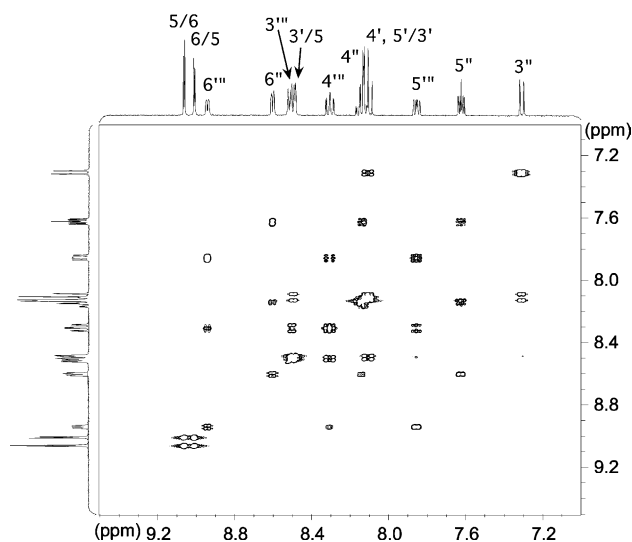

Fig. 4. Pulsed field gradient ^{1}H–^{1}H correlation spectrum for **1aZnCl$_2$** (CD$_3$NO$_2$, 400 MHz).

on the Jeol 270 GSX instrument. All NMR spectra were referred to Me₄Si at δ 0.0 ppm. Except for diketone **2**, all starting materials and solvents were commercially available and used without further purification.

4.2. Syntheses

4.2.1. Ligand 1b

To a solution of diketone **2** [8] (0.30 g, 1.0 mmol) in AcOH (15 ml) was added diaminomaleonitrile (0.10 g, 1.0 mmol). The reaction was refluxed for 1 h. Afterwards, the mixture was cooled to room temperature, the product extracted (CH_2Cl_2, 3×10 ml), the combined organic extracts were washed (H_2O, 3×10 ml), dried ($MgSO_4$) and the solvent removed by rotary evaporation at atmospheric pressure to give a brown solid. The product was purified by column chromatography (CH_2Cl_2:EtOAc 1:1, alumina, activity stage III) and recrystallized ($CHCl_3$/hexane) to afford colourless crystals in 67% yield. M.p. 185–186 °C; Calc. for $C_{21}H_{11}N_7$: C, 69.80; H, 3.07; N, 27.13. Found: C, 69.79; H, 3.02; N, 26.85; EI-MS (70 eV) m/z (relative intensity): 360 ([**1b**-H]$^+$, 100%); 283 ([**1b**-C_5H_4N]$^+$, 14%); 128 ([$C_8H_6N_2$]$^+$, 12%); 78 ([C_5H_4N]$^+$, 32%); v(cm^{-1}) (KBr): 2362 (C≡N); 1562 (C=C); 669 (Ar–H); ^{1}H NMR (CDCl₃, 270 MHz) δ (ppm): 8.60 (1H, br d, $J = 4.9$ Hz, H6‴); 8.47 (1H, d, $J = 7.9$ Hz, H3′/H5′); 8.33 (1H, br d, $J = 4.7$ Hz, H6″); 8.23 (1H, d, $J = 7.7$ Hz, H5′/H3′); 8.07 (1H, d, $J = 7.9$ Hz, H3″); 8.05 (1H, t, $J = 7.8$ Hz, H4′); 7.94 (1H, d, t, $J = 1.6$ 7.7 Hz, H4″); 7.51 (1H, d, t, $J = 1.6$ 7.9 Hz,

H4‴); 7.30–7.07 (2H, m, H5″, H5‴); 7.08 (1H, d, $J = 7.9$ Hz, H3‴); ^{13}C NMR (CDCl₃, 67.5 MHz) δ (ppm): 155.00 (1C, C); 154.78 (2C, C); 152.42 (1C, C); 152.28 (2C, C); 149.12 (1C, C); 149.05 (1C, C); 138.33 (1C, CH); 136.86 (1C, CH); 136.48 (1C, CH); 130.05 (1C, CH); 124.63 (1C, CH); 124.40 (2C, CH); 124.35 (1C, CH); 124.05 (1C, CH); 122.28 (1C, CH); 120.33 (1C, CH); 112.95 (2C, CN); λ_{max}(CH₃CN) (nm): 240 (log ε = 4.30); 283 (4.35); 327 (4.11).

4.2.2. 1aZnCl₂

From a stock solution of anhydrous ZnCl₂ (53.9 mg, 0.395 mmol) in MeCN (20.0 ml) was added 1.00 ml (0.0198 mmol ZnCl₂) to a solution of **1a** (6.15 mg, 0.0198 mmol) in CHCl₃ (1 ml). A white solid separated from solution. Further MeCN (2 ml) was added and the mixture heated to reflux for 1 h. The solvent was removed in vacuo and the residue recrystallized from hot nitromethane to give 7.1 mg (0.026 mmol, 80%) of clear, brick-shaped crystals after filtration and drying in vacuo. This material was also suitable for X-ray diffraction studies. M.p. 284 °C (decomp.); IR v(cm^{-1}) (KBr): 1594 (m, C=C); 1456 (s, C=C); 783 (vs, Ar–H); Calc. for $C_{19}H_{13}Cl_2N_5$ Zn: C, 50.98; H, 2.93; N, 15.65. Found: C, 50.88; H, 2.84; N, 15.31; FAB-MS (NBA) m/z 409.8 (**1a**ZnCl$^+$, 42%), 375.8 (**1a**Zn$^+$, 2%), 154 (NBA, 100%); ^{1}H NMR (400 MHz, CD₃NO₂) δ (ppm): 9.07 (d, $J = 2.5$ Hz, 1H, H-5/6), 9.01 (d, $J = 2.3$ Hz, 1H, H6/5), 8.94 (br d, $J = 5.0$ Hz, 1H, H6″), 8.60 (br d, $J = 4.8$ Hz, 1H, H6‴), 8.50 (d, t, $J = 0.8$, 8.1 Hz, 1H, H3′/5′), 8.50 (t,

Table 2
Crystal data, data collection parameters and details of structure refinement for **1aZnCl₂** and **1bZnCl₂**

Substance	**1aZnCl₂**	**1bZnCl₂**
Crystal shape	pale yellow block	yellow block
Empirical formula	$C_{19}H_{13}Cl_2N_5Zn$	$C_{23}H_{17}Cl_2N_9O_4Zn$
M	447.61	619.73
Crystal size (mm)	$0.50 \times 0.30 \times 0.30$	$0.50 \times 0.50 \times 0.50$
System	monoclinic	triclinic
Space group	$P2_1/n$	$P\bar{1}$
a (Å)	7.6358(6)	9.7292(10)
b (Å)	12.4493(8)	11.8291(12)
c (Å)	18.9321(15)	12.1358(13)
α (°)	90	91.244(8)
β (°)	100.519(9)	106.679(9)
γ (°)	90	100.429(8)
U (Å³)	1769.4(2)	1311.8(2)
Z	4	2
D_c (g cm^{-3})	1.680	1.569
T (K)	153(2)	293(2)
Θ range (°)	1.97–25.86	1.76–25.00
Measured, independent and observed reflections ($I > 2\sigma I$)	13070, 3415 and 2937	6477, 4224 and 3689
R_{int}	0.0515	0.0751
Data, restraints, parameters	3415, 0, 296	4224, 0, 354
Absorption correction	semi-empirical from equivalents	empirical
Final $R_1 (I > 2\sigma I)$	0.0251 (wR_2 0.0628)	0.0631 (wR_2 0.1586)
H-locating and refining method	localized	calculated
Largest peak and hole (e Å³)	+0.392 and −0.379	+0.921 and −1.087
Maximum and minimum transmission	0.566 and 0.411	0.755 and 0.325

$J = 7.8$ Hz, 1H, H3‴), 8.31 (d, t, $J = 1.6$, 8.0 Hz, 1H, H4″), 8.15 (d, t, $J = 1.5$, 7.8 Hz, 1H, H4″), 8.09–8.14 (m, 2H, H − 5′/3′, H4′), 7.86 (ddd, $J = 1.0$, 5.0, 8.6 Hz, 1H, H5‴), 7.62 (ddd, $J = 2.0$, 4.8, 6.8 Hz, 1H, H5″), 7.31 (dd, $J = 0.5$, 8.1 Hz, 1H, H3″).

4.2.3. *1bZnCl$_2$*

To a solution of **1b** (0.0124 g, 0.034 mmol) in degassed acetonitrile (2 ml) was added $ZnCl_2$ (0.004 g, 0.03 mmol) under N_2. After a few minutes, a white precipitate was formed. This mixture was refluxed for an hour then cooled to room temperature and the solvent evaporated to give a green solid. Recrystallization from hot nitromethane, followed by slow cooling over 24 h afforded colourless crystals suitable for X-ray diffraction studies. M.p. 290 °C (decomp.); $v(cm^{-1})$ (KBr): 1596 (C=C); 1574 (C=C); 785 (Ar–H); no absorptions from the nitrile groups were visibile; Calc. for $C_{21}H_{11}Cl_2N_7Zn(CH_3NO_2)$: C, 48.89%; H, 2.39%; N, 19.89%. Found: C, 48.71; H, 2.26; N, 19.63; ES-MS (CH_3COOH/MeCN) m/z (relative intensity): 462 ([**1b**ZnCl]$^+$, 25%), 785 ([**1b**$_2$Zn]$^+$, 100%); λ_{max}(CH_3CN) (nm): 244 (log $\varepsilon = 4.02$); 283 (3.99); 320 (3.93); ^{1}H NMR ((CD_3)$_2$SO, 270 MHz) δ (ppm) 8,61 (br d, $J = 4.7$ Hz, 1H, H6″), 8.41 (dd, $J = 1.9$, 7.2 Hz, 1H, H3′/5′), 8.34 (br d, $J = 5.1$ Hz, 1H, H6‴), 8.14–8.23 (m, 2H, H4′, H5′/3′), 8.04–8.12 (m, 2H, H3‴, H4‴), 7.67 (d, t, $J = 1.7$, 7.6 Hz, 1H, H4″), 7.35–7.44 (m, 2H, H5″, H5‴), 7.04 (d, $J = 8.0$ Hz, 1H, H3″).

4.3. Crystal structure determination and data collection

Data collection occurred on a Stoe Image Plate Diffraction system, using graphite-monochromated Mo Kα radiation ($\lambda = 0.71073$ Å). Image plate distance: 70 mm, ϕ oscillation scans 0–190°, step $\Delta\phi = 1°$. The structures were solved by direct methods (SHELXS-97) and refined anisotropically on F^2 (SHELXL-97). The crystal data and particulars associated with data collection and refinement for each structure are collected in Table 2.

5. Supplementary material

CCDC-219660 (**1a**ZnCl$_2$) and CCDC-219661 (**1a**ZnCl$_2$) contain the supplementary crystallographic data for this paper. These data can be obtained free of charge at http://www.ccdc.cam.ac.uk/conts/retrieving.html or from the Cambridge Crystallographic Data Centre, 12 Union Road, Cambridge CB2 1EZ, UK (fax: +44-1223-336033; e-mail: deposit@ccdc.cam.ac.uk).

References

[1] F. Heirtzler, T. Weyhermüller, J. Chem. Soc., Dalton Trans. (1997) 3653.
[2] T. Bark, T. Weyhermüller, F. Heirtzler, Chem. Commun. (1998) 1475.
[3] P.J. Cragg, F.R. Heirtzler, M.J. Howard, I. Prokes, T. Weyhermüller, in press.
[4] F. Heirtzler, S.I.G. Dias, M. Neuburger, in press.
[5] F.R. Heirtzler, M. Neuburger, M. Zehnder, E.C. Constable, Liebigs Ann.-Recl. (1997) 297.
[6] F.R. Heirtzler, Chimia 53 (1999) 204.
[7] F. Heirtzler, M. Neuberger, K. Kulike, J. Chem. Soc., Perkin Trans. 1 (2002) 809.
[8] F.R. Heirtzler, Synlett (1999) 1203.
[9] D. Roberto, F. Tessore, R. Ugo, S. Bruni, A. Manfredi, S. Quici, Chem. Commun. (2002) 846.
[10] A. Hilton, T. Renouard, O. Maury, H. Le Bozec, I. Ledoux, J. Zyss, Chem. Commun. (1999) 2521.
[11] W.B. Lin, L. Ma, O.R. Evans, Chem. Commun. (2000) 2263.
[12] T. Salditt, Q.R. An, A. Plech, J. Peisl, C. Eschbaumer, C.H. Weidl, U.S. Schubert, Thin Solid Films 354 (1999) 208.
[13] S. Aitipamula, P.K. Thallapally, R. Thaimattam, M. Jaskolski, G.R. Desiraju, Org. Lett. 4 (2002) 921.
[14] G.R. Desiraju, J. Mol. Struct. 374 (1998) 191.
[15] S.P. Anthony, T.P. Radhakrishnan, Chem. Commun. (2001) 931.
[16] A. Jouaiti, M.W. Hosseini, N. Kyritsakas, Chem. Commun. (2002) 1898.
[17] A. Neels, H. Stoeckli-Evans, Inorg. Chem. 38 (1999) 6164.
[18] T. Bark, M. Duggeli, H. Stoeckli-Evans, A. von Zelewsky, Angew. Chem., Int. Ed. 40 (2001) 2848.
[19] J.D. Wright, Molecular Crystals, Cambridge University Press, Cambridge, 1995.
[20] A. Bilyk, M.M. Harding, P. Turner, T.W. Hambley, J. Chem. Soc., Dalton Trans. (1994) 2783.
[21] A. Bilyk, M.M. Harding, P. Turner, T.W. Hambley, J. Chem. Soc., Dalton Trans. (1995) 2549.
[22] C.E. Housecroft, A.G. Sharpe, Inorganic Chemistry, Prentice Hall, Harlow, 2000.
[23] D.S. Reddy, Y.E. Ovchinnikov, O.V. Shishkin, Y.T. Struchkov, G.R. Desiraju, J. Am. Chem. Soc. 118 (1996) 4085.
[24] B.L.V. Prasad, H. Sato, T. Enoki, S. Cohen, T.P. Radhakrishnan, J. Chem. Soc., Dalton Trans. (1999) 25.
[25] J.H. Kim, S.R. Shin, M. Matsuoka, K. Fukunishi, Dyes Pigm. 41 (1999) 183.
[26] J.Y. Jaung, M. Matsuoka, K. Fukunishi, Synthesis (1998) 1347.
[27] R. Taylor, O. Kennard, J. Am. Chem. Soc. 104 (1982) 5063.
[28] C.A. Hunter, J.K.M. Sanders, J. Am. Chem. Soc. 112 (1990) 5525.
[29] F.R. Heirtzler, M. Neuburger, M. Zehnder, S.J. Bird, K.G. Orrell, V. Sik, J. Chem. Soc., Dalton Trans. (1999) 565.
[30] F. Heirtzler, P. Jones, M. Neuburger, M. Zehnder, Polyhedron 18 (1999) 601.